GD 95

TOKYO

PROCEEDINGS OF

THE ELEVENTH INTERNATIONAL CONFERENCE ON

GAS DISCHARGES AND THEIR APPLICATIONS

Volume I

CHUO UNIVESITY, 11-15 September 1995

Organised by

The Institute of Electrical Engineers of Japan

All the papers in the Proceedings were reviewed by the Local Programme Committee.

The Eleventh International Conference on Gas Discharges and Their Applications

Chuo University, Tokyo, 11-15 September 1995

GD 95

FUNDAMENTAL PROCESSES IN GAS DISCHARGES

L. G. Christophorou[1,2], R. J. Van Brunt[2] and J. K. Olthoff[2]

[1] Department of Physics, The University of Tennessee, Knoxville, TN 37996
[2] Electricity Division, Electrical and Electronics Engineering Laboratory, National Institute of Standards and Technology, Gaithersburg, MD 20899

ABSTRACT

Recent aspects of fundamental processes in gas discharges are discussed. These include the effect of internal energy of excitation of atoms and molecules on their interactions with slow electrons, the effect of temperature on electron attachment and detachment processes, photodissociation of molecules and photodetachment of anions, and interactions involved in discharge byproduct formation and discharge diagnostics. Reference is also made to fundamental processes in gas discharge materials used in plasma processing.

INTRODUCTION

In this paper an overview is given of recent developments in identifying fundamental processes underpinning the behavior of gas discharges and their applications. Many such processes involve neutral species, positive and negative ions, electrons, and photons. Collectively these processes control the behavior and characteristics of the discharge and its uses. While the study of such processes traces back many decades, fundamental advances have been made recently in certain areas which open up new possibilities, both basic and applied. These are the ones this paper focusses on. We especially emphasize the following: (i) the effect of internal energy of excitation of atoms and molecules on their interactions with slow electrons, (ii) the effect of temperature (rovibrational energy for molecules) on their electron attachment and detachment properties, (iii) photon-molecule and photon-anion interactions and the study of radicals, (iv) basic interactions involved in discharge byproduct formation and discharge diagnostics, and (v) the effect of the medium on fundamental reactions. Reference is also made to a few recent findings on fundamental processes in gas discharge materials used in plasma processing (e.g., silane and halocarbons).

EFFECT OF INTERNAL ENERGY OF EXCITATION OF ATOMS AND MOLECULES ON THEIR INTERACTIONS WITH SLOW ELECTRONS

The interactions of slow electrons with atoms and molecules are functions of not only the kinetic energy of the electron and the target atom or molecule, but also of the internal energy of the latter. While the study of the interactions of slow electrons with ground state atoms and molecules traces back many decades, the study of the interactions of slow electrons with excited atoms and molecules as a function of their internal energy (electronic and/or rovibrational for molecules) is more recent and more limited. In the past, experimental studies on electron-excited target interactions have been difficult because, the excited species are often short-lived and chemically reactive and because it is difficult to produce sufficient numbers of excited species to study under controlled conditions. Today, however, such studies are becoming increasingly more feasible through the use lasers.

Excited species are of interest in gas discharges (for instance, the importance of the formation and destruction of rare-gas-atom metastables has long been recognized). Recent studies, referred to in this paper, have shown that the cross sections for electron-atom/molecule interactions depend rather strongly on the internal energy content of the atom/molecule and in many instances the cross sections are several orders of magnitude larger than for the ground states, and hence even a small percentage of excited species present in the discharge can alter its behavior. Such knowledge on electron-excited atom/molecule interactions offers unique opportunities for changing the electrical properties of gaseous matter by the use of lasers and has potential applications in other applied areas such as in the development of ultrasensitive analytical instruments.

Examples of these new reactions are given in this section (see, also [1-3]). The limited experimental and theoretical studies to date on slow electron-excited atom/molecule collisions show many and often profound changes in the cross sections for electron scattering, ionization, attachment and detachment. Especially profound are the reported increases in the cross sections for electron scattering from electronically excited atoms and the cross sections for dissociative electron attachment to electronically excited molecules.

Electron Scattering from Excited Atoms and Molecules

In Fig. 1 are compared [4] the total electron scattering cross sections for the ground state CO_2 and for the vibrationally excited CO_2 molecules [mostly in the low-lying (0.083 eV) 01^10 bending mode]. The bending CO_2 vibration has an associated electric dipole moment and it was suggested [4] that the enhancement in the electron scattering cross section is due to the electron-electric dipole moment interaction associated with this bond. The cross sections for slow electron-electric dipole scattering are known to be large [5].

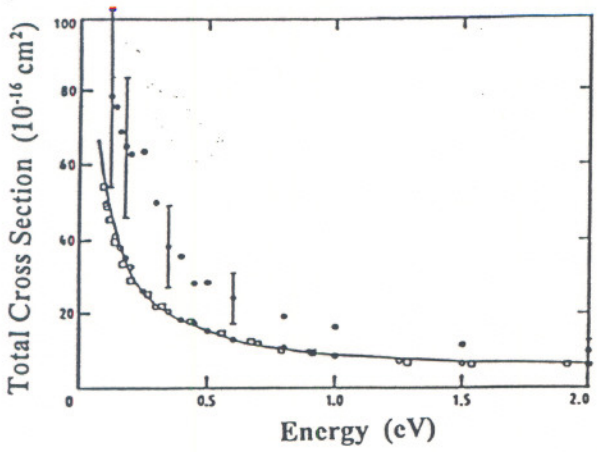

Fig.1 Total cross section for electron scattering from CO_2 in the energy range 0 to 2 eV: (.) vibrationally excited, (o,o, ——) ground state ([1],[4a])

However significant the effects of vibrational excitation on the cross section for electron scattering are, they are much smaller compared to those involving electronically excited atoms and molecules. This can be seen (Fig.2) from the measurements on singlet O_2 where the cross section for excitation of the $b^1\Sigma^+_g$ state of O_2 from the excited state $O_2^*(a^1\Delta_g)$ is more than ten times larger than from the ground state $O_2(X^3\Sigma^-_g)$ [6] . It is further dramatized by the more extensive data on excited atoms (Figs. 3 and 4).

In Fig. 3 are compared the momentum transfer cross section, σ_m , for electron-ground state argon atom [Ar($3\ ^1S$)] scattering [7] with the cross section for elastic scattering of electrons from the excited argon atom $Ar^*(4^3P_2)$, σ^*_e , calculated by Robinson [8]; the latter cross section exceeds the former substantially [around the Ramsauer-Townsend (R-T) minimum by about 10^4 times]. The R-T minimum -- so prominent a feature in the cross section for electron scattering from the ground state of the heavier rare gas atoms -- is entirely absent from the cross sections for electron scattering from the excited state(s) of the rare gas atoms. This is a consequence of the much larger electric dipole polarizability, α, of the excited state ($\alpha = 318.2\ a_o^3$ [9]; a_o = Bohr radius) compared to that of the ground state atom ($\alpha = 11.07\ a_o^3$ [9]), and the resultant dominant role of the electron-induced dipole polarization potential in the scattering. The results of a number of calculations clearly show that the cross sections for scattering of slow electrons from excited atoms are large and that they are characterized by a large contribution of higher angular momenta, L, to the total cross section as opposed to the cross sections for electron scattering by ground-state atoms where most of the contributing partial waves have small L values.

The dominant role of the dipole polarizability in electron scattering can be seen from the measurements of the differential electron scattering cross sections from ground and excited atoms. Thus, measurements [10] of the differential electron scattering cross section for excitation by 30 eV electrons of the 2^3P excited state of He from the metastable state 2^3S and from the ground state (1^1S) of He showed (Fig.4) that the cross section for the excited state is up to 10^5 times larger compared to the ground state. The maximum enhancement is for small angles (forward scattering) as is to be expected for the distant

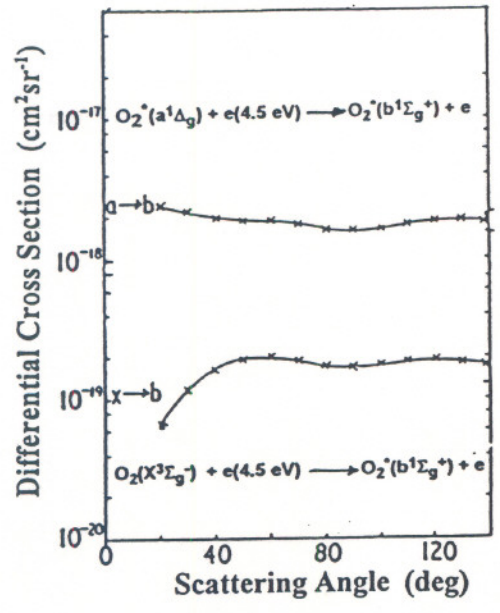

Fig. 2 Differential cross sections for 4.5 eV electrons on ground [$O_2(X^3\Sigma_g^-)$] and excited [$O_2^*(a^1\Delta_g)$] oxygen molecules [6]

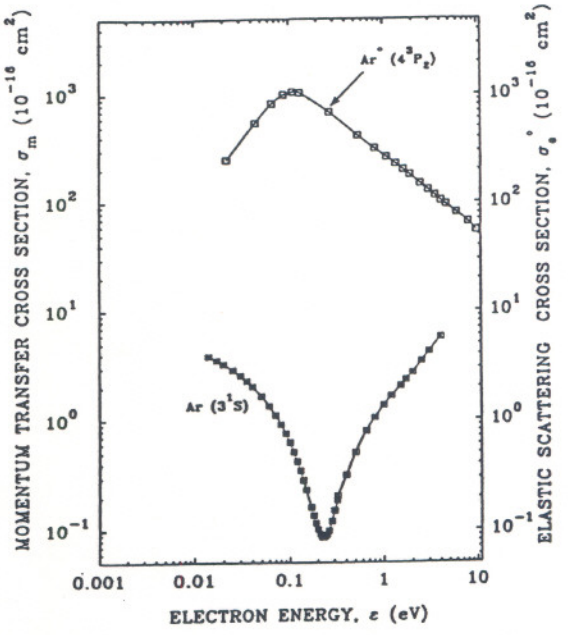

Fig. 3 Comparison of the momentum transfer cross section for scattering from the ground state argon atom Ar (3^1S) with the elastic electron scattering cross section from the excited argon atom $Ar^*(4^3P_2)$ (see the text)

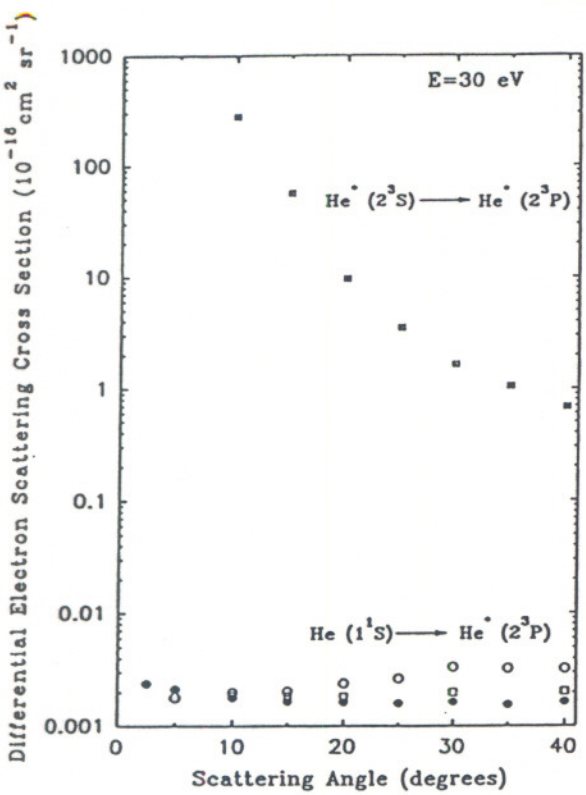

Fig. 4 Differential electron scattering cross section as a function of scattering angle for the excitation of the 2^3P state of He from the excited state 2^3S (see [10]) and from the ground state 1^1S (from [2]) of the He atom by 30 eV electrons

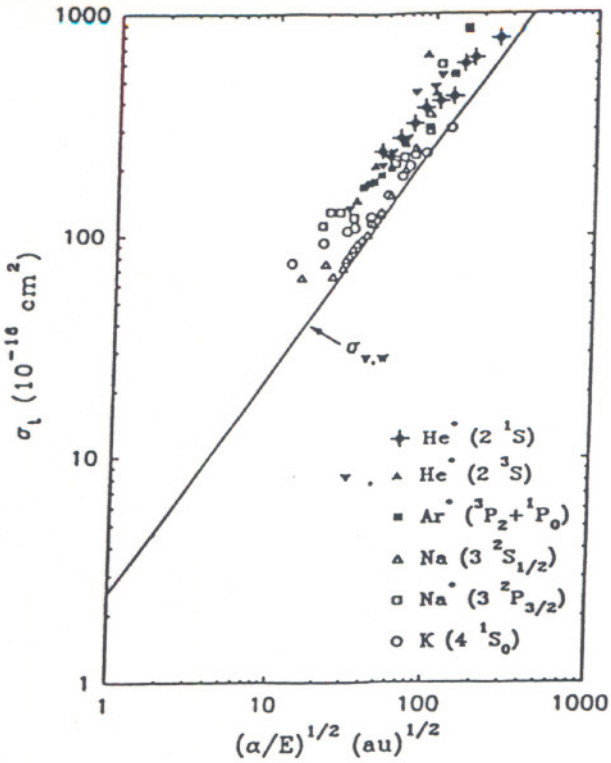

Fig. 5 Total electron scattering cross section plotted versus (α /ε)$^{1/2}$ for a number of ground state and excited atoms (see the text and [9])

collisions involved in the electron-induced dipole scattering ([α(He (1^1S)] = 1.38 a_0^3 ; α(He*(2^3S) = 315 a_0^3 [9]). Actually, it has been shown [9] that the Vogt-Wannier "limiting case formula"

$$\sigma_{V,W} = 2.487\times10^{-16}\,(\alpha/\varepsilon)^{1/2} \qquad (1)$$

(where α and the electron energy,ε, are in atomic units and $\sigma_{V,W}$ in cm^2), obtained by considering the interaction between an electron and an atom to be simply the polarization function [11]

$$V(R) = -1/2\,(e^2\alpha/R^4) \qquad (2)$$

predicts reasonably well the magnitude of the total scattering cross section (see Fig. 5). Clearly the large electron scattering cross sections for the excited states are largely due to the large α of the excited atoms (see, also, [1] and [2]).

Electron Impact Ionization of Excited Atoms and Molecules

There are no data that we know of on the electron impact ionization cross section σ_i of *vibrationally* excited molecules and those on *electronically* excited molecules are very limited [1,12]. In Fig. 6 are presented the results of a binary encounter approximation calculation [12b] for ionization of the metastables

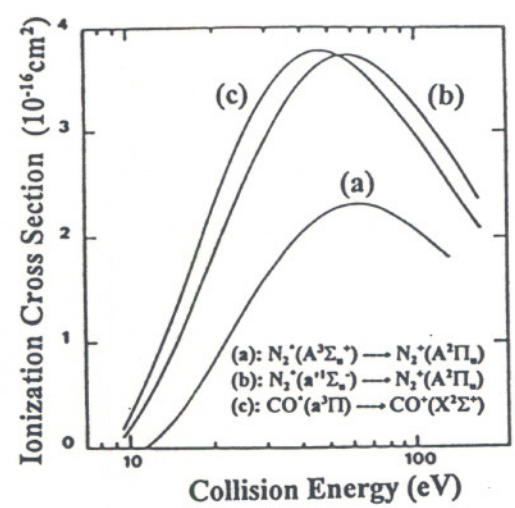

Fig. 6 Calculated electron impact ionization cross sections for the metastables $N_2^*(A^3\Sigma_u^+)$, $N_2^*(a'\ ^1\Sigma_u^-)$ and $CO^*(a^3\Pi)$ (from [12b])

$N^*_2(A^3\Sigma^+_u)$, $N^*_2(a'^1\Sigma^-_u)$ and $CO^*(a^3\Pi)$. These are generally higher than those for the corresponding ground state species; the peak values of the total ionization cross section for the ground state molecules are 2.5x10^{-16} cm^2 for N_2 and

2.6×10^{-16} cm^2 for CO [13]. Both theory and experiment have shown [2] that σ_i is larger for excited atoms compared to ground state atoms as can be seen from Fig. 7; the lower ionization thresholds and the higher dipole polarizabilities of the excited species cause a shift of the cross section maximum to lower energies which, in turn, affects the rate coefficients of the various discharge processes.

Electron Attachment to Excited Molecules

The internal energy of molecules plays a crucial role in determining their electron attachment (and detachment, see next Section) properties [1,3,16]. It has been known for sometime (e.g., see [1,3,5,16]) that the cross sections for *dissociative electron attachment* to "hot" (rovibrationally excited molecules) can be very much larger than for the ground state molecules. The increase is a function of the internal energy of the molecule and the relative positions of the potential energy curves (surfaces) of the dissociating negative ion state and the ground state; as the internal energy of the molecule increases, lower energy electrons are captured for which the cross sections are larger and the resultant transient anions dissociate faster. A recent example of such profound effects is shown in Fig. 8 [17]. It has, also, been known that *nondissociative electron attachment* to hot molecules decreases with increasing temperature due to enhanced autodetachment of the transient anion as its internal energy is increased [3,18].
The effect of temperature on electron attachment and detachment processes has been well studied recently with a number of new techniques. In Fig. 9 is depicted the principle of one such new method, namely the *time-resolved electron swarm technique* [18]. This technique allows information on electron attachment and detachment processes to be obtained simultaneously from an analysis of transient electron waveforms. The electron swarm is produced by a narrow N_2 laser pulse

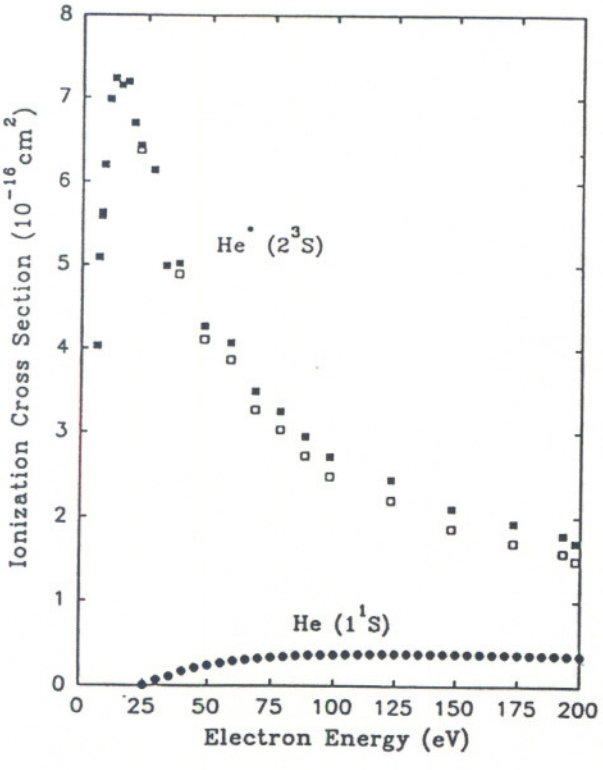

Fig. 7 Electron impact ionization cross section of the ground-state helium atom He(1^1S) (., [14]) and the excited helium He*(2^3S) (○, ■, [15])

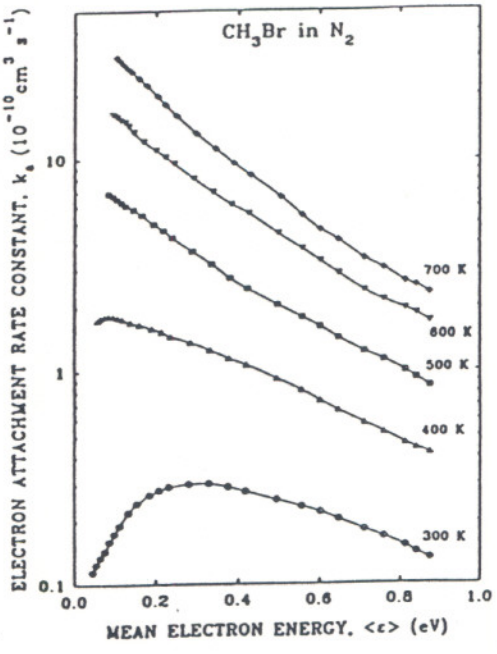

Fig. 8 Total dissociative electron attachment rate constant for CH_3Br as a function of the mean electron energy at various temperatures [17]

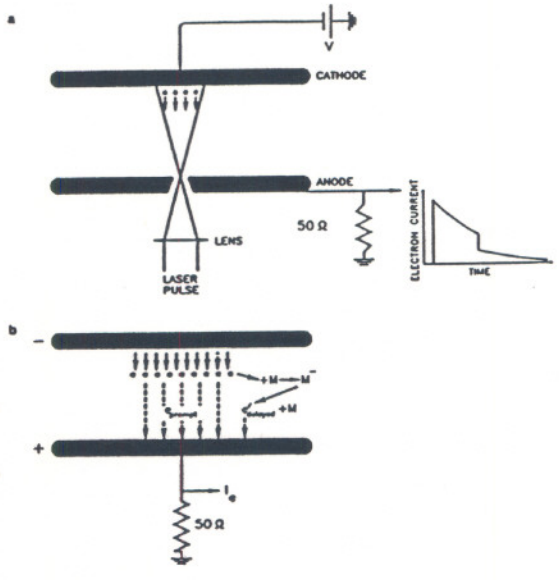

Fig. 9 Schematic diagram of the principle of the time-resolved electron swarm technique (see [18] for details)

which strikes the cathode electrode through a hole in the anode electrode. The electrons drift to the anode under the influence of an applied electric field. As they drift a fraction is removed by attachment forming unstable negative ions which are quickly stabilized by collisions with the buffer gas, forming stable negative ions. Subsequently, these stabilized anions are thermally autodetached giving rise to delayed electrons. The motion of those electrons which reach the anode without ever been attached ("prompt" electrons) and those electrons which have been captured and then released ("delayed" electrons) induces a current in the anode circuit which is observed through a 50 Ω resistor to the ground. The electron current is given by [18,19]

$$i_e(t) = e w_e / d \int_{w_i t}^{\min(w_e t, d)} \rho_e(x,t)\, dx \qquad (3)$$

where $\rho_e(x,t)$ is the electron number density; w_e and w_i are the electron and ion drift velocities and d is the drift distance. An example of the recorded waveforms as they were obtained for c-$C_4F_6^-$ is shown in Fig. 10. The solid curves [curve 1; Fig.10d] are the experimentally measured total electron currents as a function of time; the dash-dot curves [curve 2; Fig.10d] are the calculated electron current waveforms for the t_a^{-1} and t_d^{-1} obtained from a fit to Eq. 3 and the values of t_a^{-1} and t_d^{-1} given in the figure to curves 1; the dotted curves [curve 3; Fig.10d] represent the contribution to the total electron current of the initial (prompt) electron swarm when only electron attachment occurs, and the broken curves [curve 4; Fig. 10d] represent the contribution to the total electron current from the autodetached ("delayed") electrons. As T is increased this latter contribution becomes increasingly more significant; the parent anions autodetach faster. From recorded electron current waveforms such as in Fig. 10, the electron attachment frequency t_a^{-1} and the electron detachment frequency t_d^{-1} are obtained at each temperature using a nonlinear least squares fit; $t_a^{-1} = k_a N_a$ where k_a is the nondissociative electron attachment rate constant and N_a is the attaching gas number density. In Figs. 11a and 11b are shown, respectively, the k_a for c-$C_4F_6^-$ formation and the t_d^{-1} for c-$C_4F_6^-$ destruction by electron autoejection as a function of the mean electron energy and the gas temperature. Clearly while the electron attachment rate constant is little affected by increasing T above ambient, the electron detachment frequency t_d^{-1} is increased dramatically as T is raised from 450 to 600 K. The latter is also shown in Fig. 11c where t_d^{-1} is plotted as a function of the internal energy of the c-$C_4F_6^-$ anion. The heat-enhanced autodetachment has an activation energy of 0.237 eV for c-$C_4F_6^-$ and 0.477 eV for $C_6F_6^-$ [18]; it is a strong function of the electron affinity of the molecule. Thus, in sharp contrast to the profound increases in the thermally-induced autodestruction of the parent anions c-$C_4F_6^-$ and $C_6F_6^-$ with increasing T, no thermally-induced autodetachment was observed for SF_6^- up to 600 K. This is understood on the basis of the larger electron affinity (1.05 eV [20]) of the SF_6 molecule. At least up to 600 K, the collisionally stabilized SF_6^- is stable with respect to autodetachment ($t_d^{-1} < 0.001 \times 10^6\ s^{-1}$ [18]).

On the basis of these results, then, it can be concluded that there is littlte effect of T on the k_a of parent anion formation but there is a profound effect of T on the autodetachment frequency which increases with T; this increase, however, depends rather strongly on the binding of the extra electron in the anion. These findings are significant for the modelling of gas discharges and for understanding the behavior of gaseous dielectrics especially under conditions where electron detachment is a source of gas-breakdown-initiating electrons.

Recent studies [3,21] on electron attachment to electronically excited molecules--prepared by laser light prior to or concomitantly with the generation of the attaching electrons--have shown that the cross section for *dissociative electron attachment* to electronically excited molecules can be orders of magnitude larger than for the ground state molecules. A number of techniques have been developed for these studies and their principle is shown in Fig.12.

The first group (Figs 12a-c) deals with electron attachment to excited electronic states-- poduced directly or indirectly from higher-lying excited states reached initially by single or multiple photon absorption-- studied in high pressure (1 to 100 kPa) gas mixtures using a pulsed Townsend technique [21a,b,c]. In Fig. 12a, a laser pulse enters the interaction region through the gridded bottom electrode, produces excited molecules M^* in the interaction region, and generates a pulse of electrons at the top electrode. The electron swarm reaches a known steady-state energy distribution within $<10^{-8}$ s, and drifts through the partially excited gas. The drift time taken by the electrons to reach the bottom electrode is $< 10^{-5}$ s, and thus electron attachment to the excited states can take place if the lifetime τ of the excited molecules is $> 10^{-5}$ s.

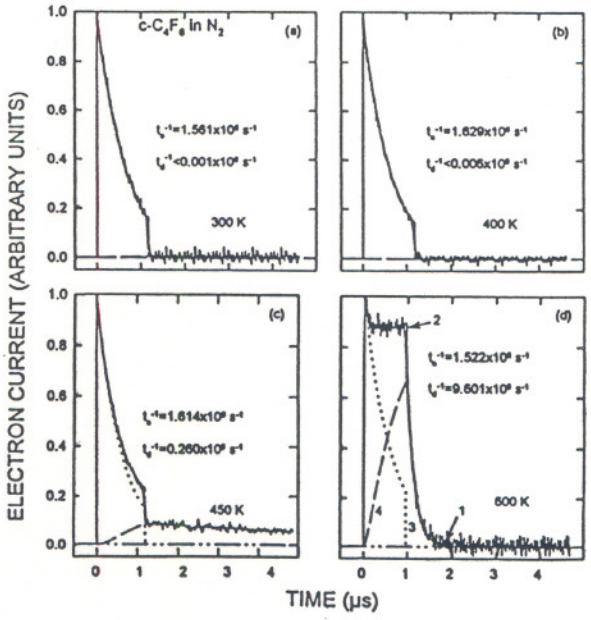

Fig. 10 Electron current waveforms for c-C_4F_6 in N_2 at T = 300, 400, 450 and 600 K. All waveforms are for E/N = 1.24×10^{-17} Vcm^2; $N_T = 6.44 \times 10^{19}$ molecules cm^{-3} [18]

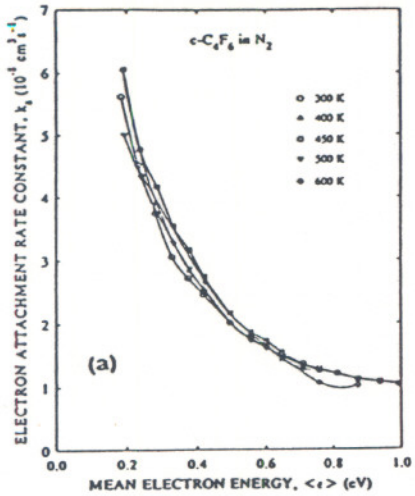

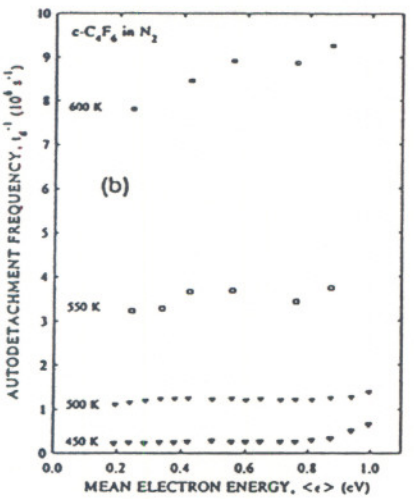

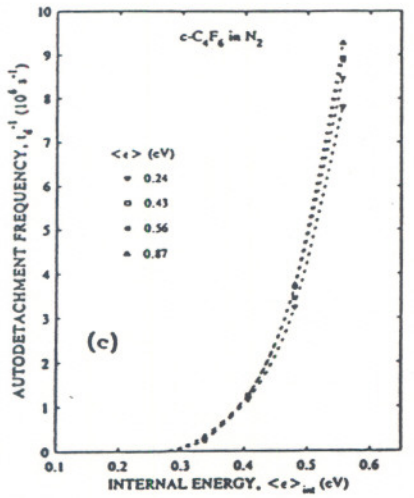

Fig. 11 a. Electron attachment rate constant k_a for c-C_4F_6 as a function of the mean electron energy ,$<\varepsilon>$, at various temperatures

b. Autodetachment frequency t_d^{-1} for c-$C_4F_6^-$ as a function of the mean electron energy at 450, 500, 550 and 600 K.

c. Autodetachment frequency t_d^{-1} for c-$C_4F_6^-$ as a function of the internal energy of the anion for four values of the mean electron energy [18]

ELECTRON ATTACHMENT TO ELECTRONICALLY-EXCITED MOLECULES

Electron Swarm Experiments:

--Electrons brought to the excited molecules M^* within $\tau_M^*(\geq 10^{-5}\ s)$

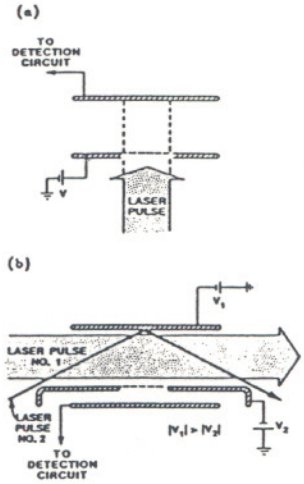

-- Electrons produced concomitantly with and in the vicinity of $M^*(\tau_M^* < 10^{-8}\ s)$

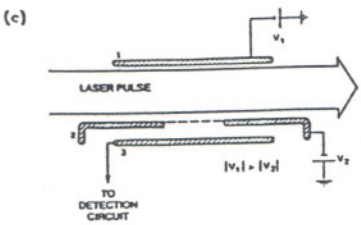

Electron Beam Experiments

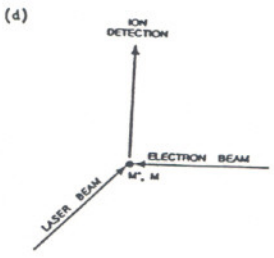

--Proper Synchronization of laser and electron beams

$-\tau_{detection} < \text{min.}\ \{\ \tau_M^*\ ;\ \tau_{diffusion}\ \}$

Fig. 12 Principles of novel electron swarm and electron beam techniques for the study of electron attachment to electronically excited molecules (see the text and [3],[21])

The arrangement of Fig.12b is an improved version of that in Fig. 12a. The production of excited species is decoupled from that of the attaching electrons by using two lasers as shown; thus the time delay between the production of the excited species and the arrival of the attaching electrons in the interaction region can be varied. Furthermore, the use of three electrodes for separating the interaction and the detection regions allows the detection of negatively charged particles unambiguously.
In these two arrangements the electrons are brought to the excited molecules M^* within the lifetime τ_M^* of M^* which must be > 10^{-5} s. By contrast, in Fig. 12c the principle of another swarm technique is illustrated which has been developed [21 b,c] to measure electron attachment to short-lived excited states ($\tau_M^* < 10^{-8}$ s) in a high-pressure (1 to100 kPa) environment. The electrons are produced concomitantly with and in the vicinity of the excited molecules M^* (via photoionization of the same gas under study or a suitable additive gas) by a single laser pulse (Fig.12c). Since the excited species and the electrons are produced in close proximity, electron attachment can occur in spite of the short τ_M^*.
The second group of techniques (Fig. 12d) deals with long-lived ($\tau_M^* > 10^{-5}$ s) excited electronic states under single collision conditions (pressures < 10^{-4} torr) using electron beams and pulsed lasers. They require proper synchronization of the laser and the electron beams. In the only such experimental study to date [21d], the electron beam was continuous and the laser beam was an excimer laser pulse having repetition rates of < 150 Hz. In this experiment it was important to selectively detect negative ions arriving at the detector within a particular gate time $\Delta\tau_G$ after a preset delay time τ_D from each laser pulse. The gate delay is associated with the time taken by the (laser-initiated) negative ions to arrive at the detector, and the gate time should be < minimum (τ_M^*, τ_D), where τ_M^* is the lifetime of the excited molecules and τ_D is the time taken by the excited molecules to diffuse out of the interaction region. (See details in [3, 21d]).

Examples of the new information obtained by these three types of novel experiments represented by Figs 12a,b, Fig. 12c, and Fig. 12d are shown, respectively, in Figs 13, 14, and 15. In Fig. 13 is shown the first [21a] observation of optically enhanced dissociative electron attachment to electronically excited states. Curve 1 is the coefficient for dissociative electron attachment to the thiophenol molecule (C_6H_5SH) in the ground state (laser off) as a function of the density reduced electric field E/N ; curve 3 is the measured coefficient for electron attachment to the thiophenol molecule in its first excited triplet state, reached indirectly from higher excited (singlet) states, themselves populated by single photon absorption using the 249 nm KrF excimer line. When the laser photon energy is below the first excited singlet state of the molecule (which is the case for the 308 nm laser line) no enhacement is observed (curve 2 in Fig. 13). The enhancement is actually about 100 times larger than indicated in the figure since the ratio of the excited to the unexcited thiophenol molecules was about 0.01 under the experimental conditions of reference 21a.
In Fig.14 are shown the large negative ion signals observed when H_2 was irradiated with the ArF laser line (192 nm) and its dependence on the laser intensity I. Virtually no anions are formed from ground state H_2 at room temperature; the rate constant for H^- production at 3.75 eV is < 10^{-14} cm^3s^{-1} (see p. 455 of [5]). The large negative ion signals under laser irradiation were interpreted as resulting from electron attachment to high-

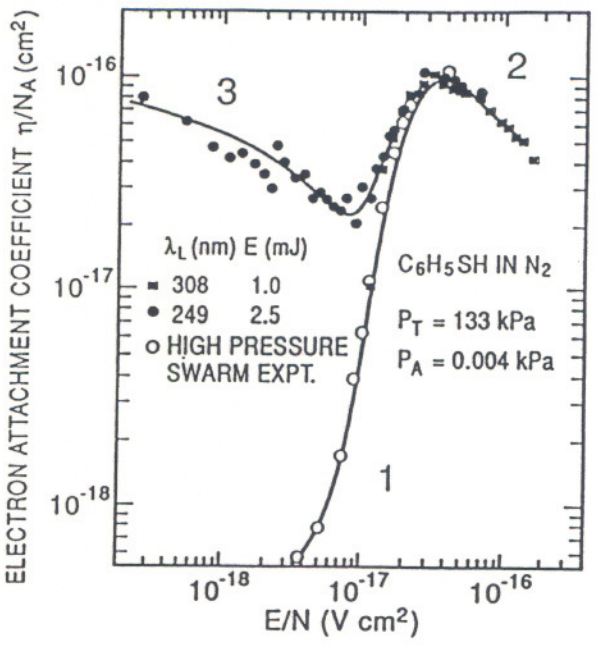

Fig. 13 Electron attachment coefficient η/N_a versus E/N for C_6H_5SH in N_2 for the ground state (curves 1 and 2) and the first excited triplet state (curve 3) of the molecule [21a]

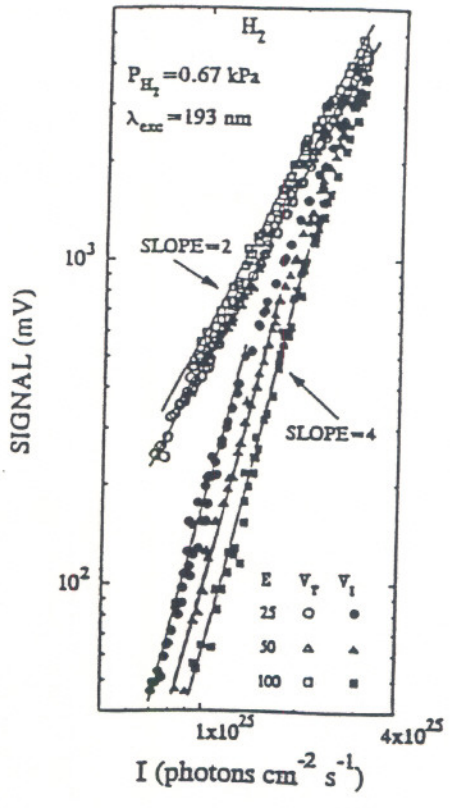

Fig. 14 Laser intensity ,I, dependence of the measured total (V_T) and negative ion(V_I) signal for H_2 under the experimental conditions shown in the figure (see the text and [21c])

lying excited states of H_2 which are reached by three-photon absorption; they indicated that the rate eonstants for electron attachment to such states (or to lower-lying excited states to which these decay) are enormous: > 10^{-6} cm^3s^{-1} [21c,22]. Cross sections of such magnitude can have profound implications in many technologies (e.g., negative ion and neutral particle beams [22], H_2 discharges [23], lasing mechanisms [24]). The observation of laser enhanced dissociative electron attachment to SiH_4 [25], CH_4 [26] and other molecules [3] points to their possible significance in plasma deposition and materials processing and to the possible development of ultrasensitive analytical instruments.

In Fig. 15 is compared the cross section for O^- production from SO_2 in the ground state (Fig.15a) and under laser irradiation (XeCl line; 308 nm) (Fig. 15b). The O^- signal with the laser on was obtained at a laser repetition rate of 150 Hz; the rest of the experimental conditions were as for Fig. 15a. It is evident that under laser irradiation in addition to the ground-state processes (Fig. 15a) an intense peak appears at near-zero energy which was attributed [21d] to the reaction

$$h\nu(308\ nm) + SO_2 \longrightarrow SO_2^*(^1B_1 \text{ or } ^1A_2)$$
$$\xrightarrow{+ e^- (< 0.5\ eV)} SO_2^{*-} \longrightarrow O^- + SO \qquad (4)$$

The electron energy required for the transition from $SO_2^*(^1B_1$ or $^1A_2)$ to SO_2^{*-} is small, and thus the photoenhanced signal appears at close to zero energy. The photoenhanced resonance is also narrower, due to the change in the equilibrium distance of SO_2^* compared to SO_2. The broken curve in Fig. 15b is the experimental data corrected for the variation of the electron current with electron energy and normalized at 8 eV (see [21d]). The intensity of the near-zero energy peak is very much larger than is indicated in the figure because only a small fraction of the SO_2 molecules are excited by each laser pulse. The peak cross section value for the photoenhanced O^- signal was estimated [21d] to be at least 2 to 3 orders of magnitute larger than the peak cross section value (2.46×10^{-18} cm^2) for O^- from the ground state.

These observations may have implications for the behavior of SO_2 and other similar-type pollutants in the atmosphere.

PHOTON-ANION AND PHOTON-MOLECULE INTERACTIONS AND THE STUDY OF RADICALS

Photodetachment and photodissociation are two photoprocesses of interest to gas discharges. The former creates free electrons and the latter free radicals.

Photodetachment

A significant recent accomplishment has been the development of new techniques for the study of photodetachment processes in both the gas [27-31] and the other states of matter (e.g., see [30]). The method described in [30] and [31] is particularly sensitive and can provide accurate measurement of absolute photodetachment cross sections $\sigma_{pd}(\nu)$ and photodetachment energetics. In Fig.16 are presented the results of [31] for the reaction

$$SF_6^- + h\nu \longrightarrow SF_6 + e \qquad (5)$$

The photodetachment cross section has a threshold at 3.16 eV which is about three times larger than the electron affinity of the SF_6 molecule (about 1.05 eV). The magnitute of the

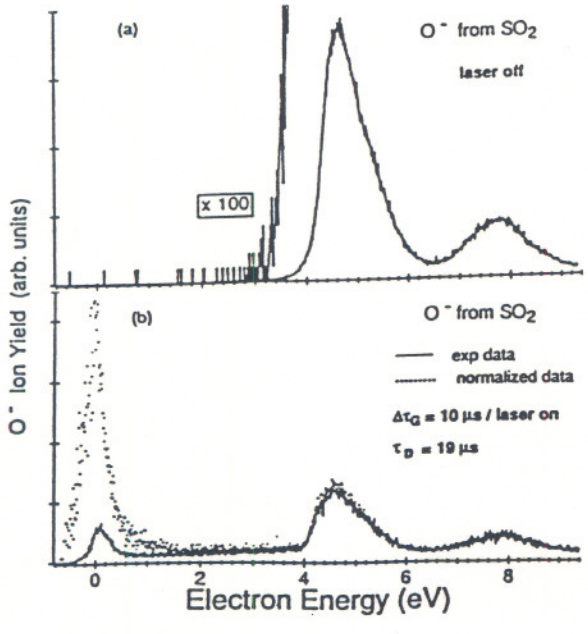

Fig. 15 Relative cross section for the production of O^- from SO_2 as a function of electron energy for ground state SO_2 molecules (Fig.15a) and for a mixture of ground and excited SO_2 molecules (Fig.15b) (See the text and [21d])

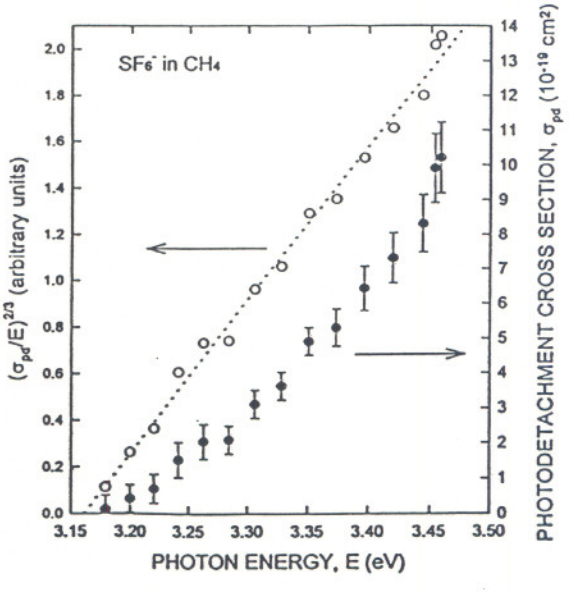

Fig. 16 (.) Photodetachment cross section $\sigma_{pd}(E)$ for SF_6^- in a buffer gas (CH_4) as a function of photon energy E. (o) A plot of $(\sigma_{pd}(E) / E)^{2/3}$ versus E consistent with a threshold value of 3.16 eV [31]

photodetachment cross section increases from the threshold to $1.0x10^{-18}$ cm^2 at a photon energy of 3.46 eV. The small size of the measured photodetachment cross section is attributed to the large relaxation in the equilibrium internuclear positions of SF_6^- compared to SF_6.

Photodissociation

A most interesting study of this fundamental process is that on the photodissociation of freons under collisionless conditions using lasers: $CHFCl_2$ [32], $CHCl_3$ [32], CF_2BrCl [33], $CFCl_3$ [34], CF_2Cl_2 [35] and the radical $CHCl_2$ [32]. These studies provided absolute cross section data and photodissociation quantum yields for specific radicals which can allow the controlled photoproduction of radicals for further study. Such investigations are important in view of the use of these freon compounds in plasma processing of materials. In Table 1 are listed pertinent findings by these workers. The high yields for the reactions given in the Table clearly show that at the laser light wavelength (193 nm) used, the decay of the excited states of these freons is via the C -Cl fission. (See, also, a review of absolute cross sections for photoabsorption, partial photoionization and ionic photofragmentation processes for a number of molecules in [36]).

Table 1: Photodissociation of freons by 193 nm laser light

Photodissociation Reaction	Photodissociation Cross Section (10^{-18} cm^2)	Photodissociation Quantum Yield	Reference
$CF_2Cl_2 + h\nu \rightarrow CF_2Cl + Cl$	~ 3.5	~1	33
$CFCl_3 + h\nu \rightarrow CFCl_2 + Cl$	14	~1	34
$CHFCl_2 + h\nu \rightarrow CHFCl + Cl$	2	~1	32
$CHCl_3 + h\nu \rightarrow CHCl_2 + Cl$	8	~1	32

Radicals

The study of radicals, especially those radicals which are of technological significance, is rather demanding. Very little is known, for example, about their electron attachment, scattering and impact ionization properties. Efforts are under way at the authors' laboratory to study electron attachment to radicals and recently significant results have been reported [37-40] on electron impact ionization of radicals of interest to plasma etching and deposition. For example, the free radicals CF_3, CF_2, and CF were prepared [37-40] by near-resonant charge transfer reactions of CF_3^+, CF_2^+ and CF^+ with various species (e.g., Xe) and the positive ions produced by electron impact on them have been identified and quantified. These radicals and their ions are most abundant and reactive species that result from the dissociation of CF_4.

In Fig. 17a are shown [37] the absolute cross sections for dissociative ionization of CF_x (x = 1-3) free radicals of CF_3; the molecular fragment ionization (CF_2^+, CF^+ from CF_3) cross section exceeds the parent ionization cross section (CF_3^+ from CF_3). In Fig. 17b are presented absolute cross sections for the parent ionization of the CF_x (x = 1-3) radicals by electron impact [38]. These results are important in modeling discharges of the CF_4 gas.

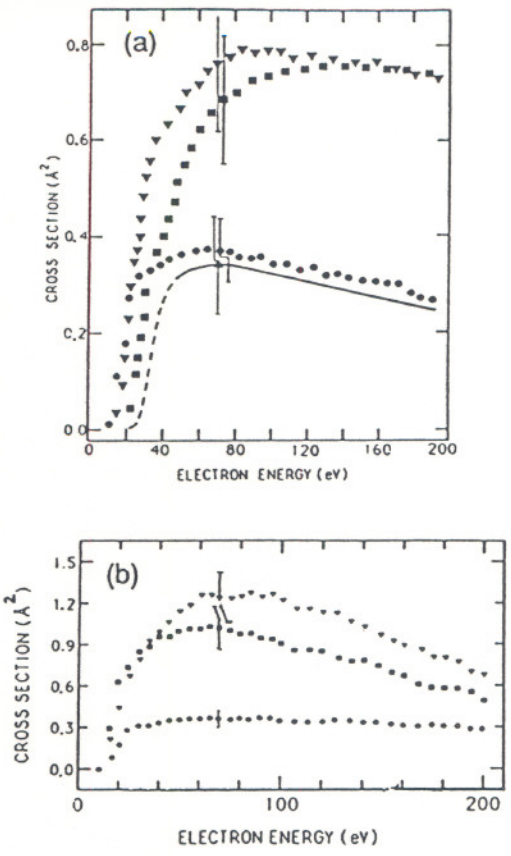

Fig. 17 a. Absolute electron-impact ionization cross section for the formation of CF_3^+ parent ions (.) and CF_2^+ (▾) and CF^+ (■) fragment ions from CF_3 as a function of electron energy. Also shown (▲) is the absolute cross section for the formation of F^- at 70 eV. The energy dependence of the F^- cross section is indicated by the solid line above 50 eV and by the broken line below 50 eV [37] b. Absolute electron- impact ionization cross section for the formation of the CF_x (x = 1 to 3) parent ions as a function of electron energy; (.) CF_3^+, (■) CF_2^+ and (▾) CF^+ (from[38]).

ANION PROCESSES INVOLVING SF_6 DISCHARGE BYPRODUCTS

When electrical discharges occur in SF_6 or in mixtures of this gas with O_2 and H_2O, a host of stable or quasi-stable electronegative byproducts are formed which include such species as SOF_2, SO_2F_2, SOF_4, SO_2, S_2OF_{10}, $S_2O_2F_{10}$, SF_4, and S_2F_{10} [41,42]. The cross sections for total electron scattering and electron attachment processes have recently been measured for these species [43-45]. Shown in Fig. 18 are the dissociative electron attachment rate coefficients as a function of E/N for SF_6, SOF_2, SO_2F_2, SF_4, and SO_2 in SF_6 which were calculated from directly measured cross sections in an electron beam apparatus [43]. Although the dissociative attachment rates for the byproducts indicated in Fig. 18, as well as the rates for SOF_4 (not shown in the figure) fall below the values for SF_6, the rates are still high enough that the dielectric strength of SF_6 is not measurably reduced when small amounts of these compounds are present.

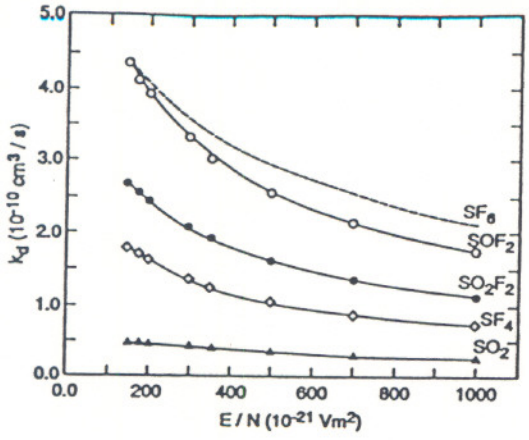

Fig. 18 Calculated total dissociative electron attachment rate coefficients for SF_6 and its discharge byproducts SOF_2, SO_2F_2, SF_4 and SO_2 in SF_6 as a function of E/N [43]

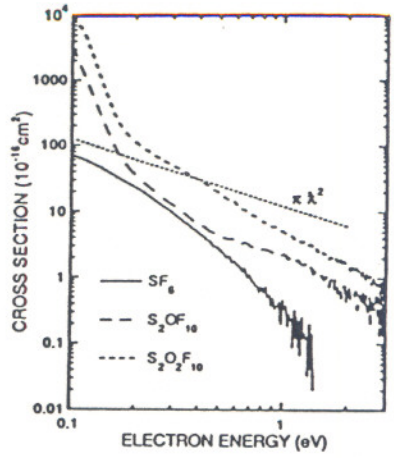

Fig. 19 Electron energy dependence of the total cross section for dissociative electron attachment to S_2OF_{10} (long dashed line), $S_2O_2F_{10}$ (short dashed line) and SF_6 (solid line) in comparison with the calculated maximum s-wave capture limit ($\pi\lambda^2$) [45]

The byproducts S_2F_{10}, S_2OF_{10}, and $S_2O_2F_{10}$, on the other hand, have electron attachment cross sections and corresponding electron attachment rate constants that are significantly higher than those for SF_6. Figure 19 shows the measured [45] electron anergy dependence of the absolute cross sections for dissociative electron attachment to S_2OF_{10}, $S_2O_2F_{10}$, and SF_6 compared to the calculated maximum s-wave capture limit ($\pi\lambda^2$) corresponding to the Wigner threshold condition [46].The cross sections for both S_2OF_{10} and $S_2O_2F_{10}$ are anomalously high, exceeding the s-wave limit at 0.1 eV by more than an order of magnitude. In the case of these molecules, there is reason to question the applicability of partial-wave analysis and therefore the s-wave limit to electron scattering because the electron-molecule interaction potentials are not likely to satisfy the requirement of spherical symmetry. It should be kept in mind that these are relatively large, asymmetric molecules that likely have multicentered interaction potentials.

The dissociative electron attachment cross section for S_2F_{10} also exhibits somewhat unusual behavior as is illustrated by the results shown in Fig. 20 which indicate a significant cross section for electron impact energies up to 11 eV. For all other SF_6 oxidation byproducts it is found that electron attachment occurs at electron energies below 8.0 eV [43,45]. The higher energy electron attachment resonances above 4 eV do not contribute significantly to the electron attachment rate for E/N less than 10^{-18} Vm^2 corresponding to typical discharge conditions in SF_6. This accounts for the relatively low rates for SO_2 seen in Fig. 18, because its ground-state dissociative electron attachment cross section is peaked near 5 eV (see Fig. 15). It is also interesting to note that SF_6^- formation contributes significantly to the S_2F_{10} dissociative attachment process at low energies below 1 eV. The experimental results [43-45] show that dissociative electron attachment is the predominant electron attachment process that occurs for all SF_6 byproducts mentioned above, and therefore, the electron attachment process will contribute to the destruction of these species in a discharge.

In assessing the role of anion processes in SF_6 discharges there are other unusual characteristics of the anion chemistry in this gas that should be pointed out. The first concerns the anomalously high collisional detachment threshold energies that have been observed [47] for the ions F^-, SF_5^-, and SF_6^- that result from electron attachment to SF_6. The measured collisional detachment cross sections for these three ions are shown in Fig. 21 and indicate that SF_6^- and SF_5^- both have detachment thresholds at about 90 eV and F^- at about 8 eV. Because of these high thresholds, the negative ions formed directly form SF_6 will not detach by collision under

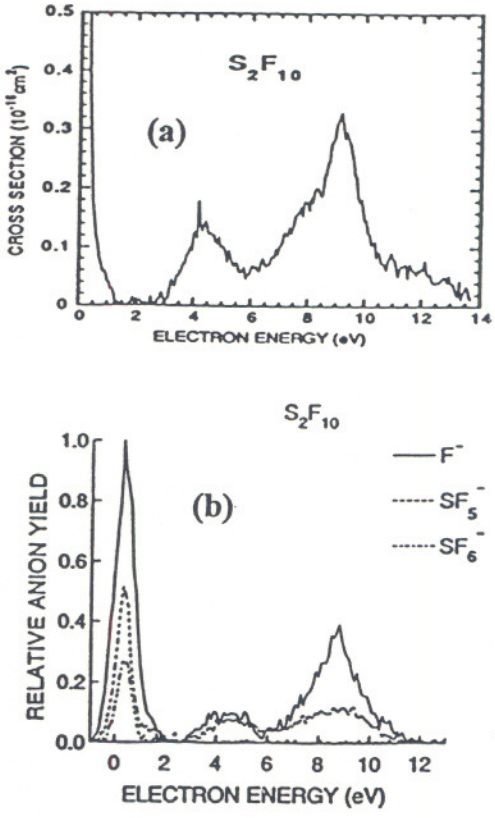

Fig. 20 a. Electron energy dependence of the cross section for dissociative electron attachment to S_2F_{10} [45]
b. Electron energy dependence of the relative anion yields from dissociative electron attachment to S_2F_{10} [45]

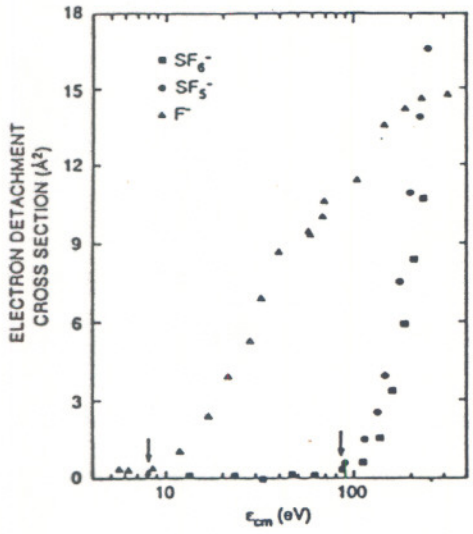

Fig. 21 Collisional electron detachment cross sections for F^-, SF_5^-, and SF_6^- on SF_6 target gas as a function of the center-of-mass energy [47]

typical discharge conditions. It can, therefore. be concluded that collisional detachment processes in SF_6 that are important for determining discharge initiation probability, will be controlled by anions associated with impurities such as OH^- from H_2O [48]. Once discharge byproducts appear in the gas, they can become important in controlling the anion chemistry through such fast reactions as:

$$SF_6^- + SOF_4 \longrightarrow SOF_5^- + SF_5$$

$$SF_6^- + SO_2 \longrightarrow SO_2F^- + SF_5$$

$$\longrightarrow SF_5^- + SO_2F$$

$$\longrightarrow SO_2F_2^- + SF_4$$

which have high rates that approach the theoretical collision limit at low temperatures or at low E/N [49, 50]. In a decomposed gas in which oxyfluoride byproducts are present, the predominant initial SF_6^- anion will rapidly convert to other ions such as SOF_5^-. At the present time, little is known about the collisional detachment rates of the oxyfluoride-type anions.

EFFECT OF MEDIUM ON GAS-PHASE REACTIONS; INTERACTIONS ON SURFACES

Many fundamental reactions depend on the density and nature of the medium in which they occur. The behavior, for example, of slow electrons in matter depends on the state of matter. In addition, the surface often acts as a catalyst and the cross sections for and energetics of reactions occurring on the surface differ from -- and affect-- those in the gas. These processes need detailed investigation as do clustering phenomena involving neutrals and/or charged particles. The topic is of current interest (e.g., see [16] and [51]).

ELECTRON SCATTERING CROSS SECTIONS FOR SILANE AND HALOCARBONS

In this section we refer to two recent studies dealing with the determination of electron scattering cross sections for polyatomic molecules of technological interest. The first study is on SiH_4 and is prototypical of the continuous effort to obtain consistent sets of low-energy electron scattering cross sections for the various elastic and inelastic processes for polyatomic molecules using electron swarm transport coefficients and Boltzmann transport equation analysis or Monte Carlo computations. In Fig.22 is shown the set of cross sections obtained recently [52] for SiH_4 by the use of Monte Carlo calculations and transport data in SiH_4-He mixtures. The authors emphasized the significance of using electron transport data on SiH_4 in a "non-Ramsauer buffer gas" (He) to achieve consistency in the derived cross sections. Cross section sets of this type are important in identifying and quantifying the precursors and the mechanisms in thin film technology using SiH_4 gas [52].

The second study is on halocarbons CF_4, $CClF_3$, CCl_2F_2, CCl_3F and CCl_4 [53] and is prototypical of efforts to measure electron scattering cross sections over wide energy ranges using monoenergetic electron beams. The measurements of this investigation on the total electron scattering cross sections from 10 to 4000 eV are shown in Fig. 23 (see, also, [54] and [55]).

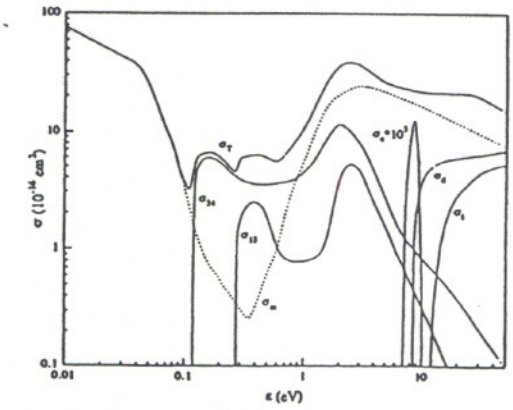

Fig. 22 Electron collision cross sections for SiH_4; the subscripts T, m, 24, 13, a, d, i correspond to the total (elastic + inelastic), momentum transfer, first vibrational, second vibrational, attachment,dissociation and ionization cross sections respectively [52].

CONCLUSION

New methods and experimental techniques provide basic knowledge which allows a deeper understanding of fundamental gas discharge processes. This knowledge opens up new possibilities for applications.

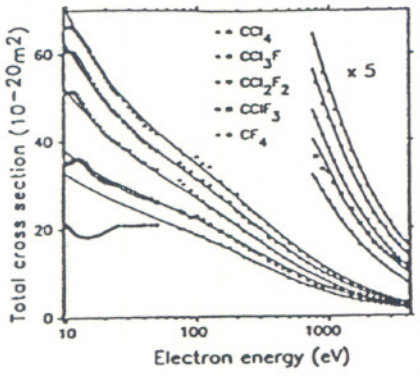

Fig. 23 Total cross sections for electron scattering from chlorofluoromethanes in the energy range 10 to 4000 eV. Points are experimental data and curves are semiempirical fits (from [53])

ACKNOWLEGEMENT

This research was sponsored in part by the Wright Laboratory, U.S. Department of the Air Force under contract AF 33615-92-C-2221 with the University of Tennessee, Knoxville, TN 37996.

REFERENCES

[1] Christophorou, L. G., In XXth Intern. Conf. on Phenomena in Ionized Gases, Palleschi, V., Singh, D. P, and Vaselli, M. , (Editors), (Pisa: Instituto di Fisica Atomica e Molecolare), Invited Papers , p. 3, 1991.

[2] Trajmar, S. and Nickel, J. C., in Adv. Atom. Mol. Opt. Phys., Bates, D. R. and Bederson, B. (Editors), Academic, Orlando, FA, p. 45, 1993.

[3] Christophorou, L. G., Pinnaduwage, L. A. and Datskos, P. G. , in Linking the Gaseous and Condensed Phases of Matter, Christophorou, L. G., Illenberger, E., and Schmidt, W. F.(Editors), Plenum, New York, p. 415, 1994.

[4] a. Buckman, S.J., Elford, M. T., Newmam, D. S., J. Phys B20, p. 5175, 1987.
b. Fersch, J., Masche, C., Raith, W., Wiemann, L. , Phys Rev. A 40, p. 5407, 1989.
c. Johnstone, W. M., Mason, N. J.and Newell, W. R., J. Phys. B 26, p. L147, 1993.

[5] Christophorou, L.G., Atomic and Molecular Radiation Physics, Wiley- Interscience, New York, 1971.

[6] Hall, R. I. and Trajmar, S., J. Phys. B 8, p. L293, 1975.

[7] Milloy, H. B. , Crompton, R. W., Rees, J. A. and Robertson, A. G., Austr. J. Phys. 30, p. 61, 1977.

[8] Robinson, E. J., Phys. Rev. 182, p. 196, 1969.

[9] Christophorou, L. G. and Illenberger, E., Phys. Lett. A173, p. 78, 1993.

[10] Muller-Fiedler, R., Schlemmer, P., Jung, K., Hotop, H. and Ehrhardt, H., J. Phys. B 17, p. 259, 1984.

[11] Vogt, E. and Wannier, G. H., Phys. Rev. 95, p. 1190, 1954.

[12] a. McCann, K. J., Flannery, M. R., and Hazi, A., Appl. Phys. Lett. 34, p. 543, 1979.
b. Ton-That, D. and Flannery, M. R., Phys. Rev. A 15, p. 517, 1977.
c. Armentrout, P. B., Tarr, S. M., Dori, A. and Freund, R. S., J. Chem. Phys. 75, p. 2786, 1981.

[13] Ref. 5, pp. 390,391.

[14] Krishnakumar, E. and Srivastava, S. K., J. Phys. B 21, p. 1055, 1988.

[15] Dixon, A. J., Harrison, M. F. A. and Smith, A. C. H., J. Phys. B 9, p.2617, 1976.

[16] Christophorou, L. G., McCorkle, D. L. and Christodoulides, A. A., in Electron-Molecule Interactions and Their Applications, Christophorou, L. G.(Editor) Academic, Orlando, FA, Vol. 1, Chapter 6, 1984.

[17] Datskos, P. G., Christophorou, L. G. and Carter, J. G., J. Chem. Phys. 97, p. 9031, 1993.

[18] a. Datskos, P. G. , Christophorou, L. G. and Carter, J. G., J. Chem. Phys. 99, p. 8607, 1993.
b. Datskos, P. G., Christophorou, L. G. and Carter, J. G., J. Chem. Phys. 98, p. 7875, 1993.
c. Christophorou, L. G. and Datskos, P. G., Intern. J. Mass Spectr. Ion Processes, in press.

[19] Wen, C. and Wetzer, J. M., IEEE Trans. Electr. Insul. 23, p. 999, 1988; 24, p. 143, 1989.

[20] Grimsrud, E. P., Chowdhury, S. and Kebarle, P., J. Chem. Phys. 83, p. 1059, 1985

[21] See, for example:
a. Christophorou, L. G., Hunter, S. R., Pinnaduwage, L. A., Carter, J. G., Christodoulides, A. A. and Spyrou, S. M., Phys. Rev. Lett. 58, p. 1316, 1987.
b. Pinnaduwage, L. A. , Christophorou, L. G. and Hunter, S. R., J. Chem. Phys. 90, p. 6275, 1989.
c. Pinnaduwage, L. A. and Christophorou, L. G., Phys. Rev. Lett. 70, p.754, 1993.
d. Jaffke, T., Hashemi. R., Christophorou, L. G., Illenberger, E., Baumgartel, H., and Pinnaduwage, L. A.,Chem. Phys. Lett. 203, p. 21, 1993.

[22] Pinnaduwage, L. A. and Christophorou, L. G., J. Appl. Phys. 76, p. 46, 1994.

[23] Garscadden, A. and Nagpal., Plasma Source Sci. Technol. (preprint, private communication, August, 1994).

[24] Kielkopf, J. F., Pinnaduwage, L. A. and Christophorou, L. G., Phys. Rev. A 49, p. 2675, 1994.

[25] Pinnaduwage, L. A., Martin, M. Z. and Christophorou, L. G., Appl. Phys. Lett. 65, p. 2571, 1994.

[26] Pinnaduwage, L. A., Martin, M. Z. and Christophorou, L. G., Contributions to Plasma Physics (submitted, February, 1995).

[27] Drzaic, P. S. and Brauman, J. I., J. Amer. Chem. Soc. 104, p. 13, 1982.

[28] Mock, R. S. and Grimsrud, E. P., Chem. Phys. Lett. 184, p. 99, 1991.

[29] Ingolfsson, O., Illenberger, E. Schmidt, W. F., Inten. J. Mass Spectr. Ion Processes 139, p. 103, 1994.

[30] Christophorou, L. G., Datskos, P. G. and Faidas, H., J. Chem. Phys. 101, p. 6728, 1994.

[31] Datskos, P. G., Carter, J. G. and Christophorou, L. G., Chem. Phys. Lett. (in press).

[32] Yang. X., Felder, P. and Huber, J. R., Chem. Phys. 189, p.127, 1994.

[33] Baum, G. and Huber, J. R., Chem. Phys. Lett. 203, p. 261, 1993.

[34] Felder, P. and Demuth, C., Chem. Phys. Lett. 208, p.21, 1993.

[35] Baum, G. and Huber, J. R., Chem. Phys. Lett. 213, p. 427, 1993.

[36] Gallagher, J. W., Brion, C. E., Samson, J. A. R. and Langhoff, P. W., J. Phys. Chem. Ref. Data 17, p. 9, 1988.

[37] Tarnovsky, V., Kurunczi, P., Rogozhnikov, D. and Becker, K., Intern. J. Mass Spectr. Ion Processes 128, p. 181, 1993.

[38] Tarnovsky, V. and Becker. K., J. Chem. Phys. 98, p.7868, 1993.

[39] Tarnovsky, V., Levin, A. and Becker, K., J. Chem. Phys. 100, p. 5626, 1994.

[40] Deutsch, H., Mark, T. D., Tarnovsky, V., Becker, K., Cornelissen, C., Cespiva, L. and Bonacic-Koutecky, V., Intern. J. Mass Spectr. Ion Processes 137, p. 77, 1994.

[41] Sauers, I., Ellis, H. W. and Christophorou, L. G., IEEE Trans. Elec. Insul. 21, p. 111, 1986.

[42] Van Brunt, R. J. and Herron, J. T., Physica Scripta T53, p. 9, 1994.

[43] Wan, H.- X., Moore, J. H., Olthoff, J. K. and Van Brunt, R. J., Plasma Chem. Plasma Proc. 13, p.1, 1993.

[44] Sauers, I., Christophorou, L. G. and Spyrou, S. M., Plasma Chem. Plasma Proc. 13, p. 17, 1993.

[45] Olthoff,J. K., Stricklett, K. L., Van Brunt, R. J., Moore, J. H., Tossell, J. A. and Sauers, I., J. Chem. Phys. 98, p. 9466, 1993.

[46] Wigner, E. P., Phys. Rev. 73, p. 1002, 1948.

[47] Olthoff, J. K., Van Brunt, R. J., Wang, Y., Champion, R. L. and Doverspike, L. D., J. Chem. Phys. 91, p. 2261, 1989.

[48] Van Brunt, R. J., J. Appl. Phys. 59, p. 2314, 1986.

[49] Sieck, L. W. and Van Brunt, R. J., J. Phys. Chem. 91, p. 708, 1988.

[50] Van Brunt, R. J., Sieck, L. W., Sauers, I. and Siddagangappa, M. C., Plasma Chem. Plasma Proc. 8, p. 225, 1988.

[51] See, for example:
a. Christophorou, L. G., Illenberger, E. and Schmidt, W. F., Editors, Linking the Gaseous and the Condensed Phases of Matter, Plenum Press, New York, 1994, and references cited therein.
b. Illenberger, E., Chem. Rev. 92, p. 1589, 1992.
c. Sanche, L., IEEE Trans. Electr. Insul. 28, p. 789, 1993.
d. Christophorou, L. G., in Physical and Chemical Mechanisms in Molecular Radiation Biology, Glass, W. A. and Varma, M. N., Editors, Plenum press, New York, p. 183, 1991.

[52] Nagpal, R. and Garscadden, A., in Gaseous Dielectrics VII, Christophorou, L. G. and James, R. D., Editors, Plenum Press, New York, p. 39, 1995; Phys. Rev. Lett. 73, p. 1598,. 1994.

[53] Zecca, A., Karwasz, G. P. and Prusa, R. S., Phys. Rev. 46, p. 3877, 1992.

[54] Szmytkowski, C., Krzysztofowicz, A. M., Janicki, P. and Rosenthal, L., Chem. Phys. Lett. 199, p. 191, 1992.

[55] Randell, J., Ziesel, J-P., Lunt, S. L., Mrotzek, G. and Field, D., J. Phys. B 26, p.3423, 1993.